

Research



Cite this article: Raffaelli M, Bohr J, Markvorsen S. 2018 Cartan ribbonization and a topological inspection. *Proc. R. Soc. A* **474**: 20170389.
<http://dx.doi.org/10.1098/rspa.2017.0389>

Received: 5 June 2017

Accepted: 5 November 2018

Subject Areas:

geometry, topology, mechanics

Keywords:

developable surfaces, ribbons, rolling, topological inspection

Author for correspondence:

Jakob Bohr

e-mail: jabo@nanotech.dtu.dk

Cartan ribbonization and a topological inspection

Matteo Raffaelli¹, Jakob Bohr² and Steen Markvorsen¹

¹DTU Compute, Department of Applied Mathematics and Computer Science, and ²DTU Nanotech, Department of Micro and Nanotechnology, Technical University of Denmark, 2800 Kongens Lyngby, Denmark

MR, 0000-0002-4908-196X; JB, 0000-0003-4076-2045; SM, 0000-0002-0061-0672

We develop the concept of Cartan ribbons together with a rolling-based method to ribbonize and approximate any given surface in space by intrinsically flat ribbons. The rolling requires that the geodesic curvature along the contact curve on the surface agrees with the geodesic curvature of the corresponding Cartan development curve. Essentially, this follows from the orientational alignment of the two co-moving Darboux frames during rolling. Using closed contact centre curves, we obtain closed approximating Cartan ribbons that contribute zero to the total curvature integral of the ribbonization. This paves the way for a particularly simple topological inspection—it is reduced to the question of how the ribbons organize their edges relative to each other. The Gauss–Bonnet theorem leads to this topological inspection of the vertices. Finally, we display two examples of ribbonizations of surfaces, namely of a torus using two ribbons and of an ellipsoid using closed curvature lines as centre curves for the ribbons.

1. Introduction

The approximation of surfaces by patchworks of planar parts has long been used in fundamental and applied mathematics, especially the multifaceted applications of triangulations [1]. In the present work, we develop a scheme for approximating a surface by the use of multiple developable surfaces. Part of the beauty of this approach is the relatively few numbers of developable stretches—ribbons—needed to approximate a given surface. Also, the study of shapes and structures of developable surfaces is itself a classical subject that has intrigued mathematicians for centuries and has found numerous artistic applications in architecture and design; see [2].

In the 1970s, Nomizu pointed out that the concept of (extrinsic) rolling can be understood as a kinematic interpretation of the (intrinsic) Levi–Civita connection and of the Cartan development of curves [3,4]. One can derive simple expressions for the components of the corresponding relative angular velocity vector of the rolling, i.e. the geodesic torsion, the normal curvature and the geodesic curvature of the given curve and its development [5–9]. For example, in conjunction with a plane, the rolling must propagate along a planar curve which has the same geodesic curvature as the given curve; see examples in [10].

In recent years, rolling has received a renewed wave of interest—in part because of its importance for robotic manipulation of objects [11]. For example, there has been an interest in understanding rolling from symmetry arguments [12] as well as purely geometrical considerations [13–15]. Also, the shapes known as D-forms are examples of surface structures that are formed by assembling several developable surfaces [16–18].

The paper is organized as follows: in §§2 and 3, we apply the notion of rolling as an alternative introduction to the construction of developable surface approximations. We show how the method of rolling a surface along the planar Cartan development of a given curve on the surface produces a planar ribbon which—after isometric bending along the lines of the instantaneous rotation axes—will reproduce the surface approximation along the said curve. In other words, the rolling induces a local isometry between the plane and the flat approximation along the curve. Further in §3, we discuss a specific measure of the local goodness of a given ribbon approximation. In §4, we then initiate the corresponding study of such approximations by establishing a precise calculation of the Euler characteristic of the surfaces via an inspection of the family of approximating ribbons. Finally, in §§5 and 6, we illustrate the approximation method by two concrete examples which show the ensuing Cartan ribbon approximations of a torus (along two trigonometric centre curves) and of an ellipsoid (along six lines of curvature), respectively.

2. The initial setting

We consider two surfaces S and \tilde{S} in \mathbb{R}^3 . Let γ be a smooth, regular curve on S , $\gamma : J = [0, \alpha] \rightarrow S$, such that $\gamma(0) = (0, 0, 0)$. We equip γ with its *Darboux frame field* $\mathcal{F} = \{e, h, N\}$, which is defined as follows: for each $t \in J$ we let $N(t)$ denote a unit normal vector to S at $\gamma(t)$ and we let $e(t) = \gamma'(t)/\|\gamma'(t)\|$ be the unit tangent vector of γ and $h(t) = N(t) \times e(t)$. The frame \mathcal{F} then satisfies the following equations (e.g. [19, corollary 17.24]):

$$\begin{bmatrix} e'(t) \\ h'(t) \\ N'(t) \end{bmatrix} = \|\gamma'(t)\| \cdot \begin{bmatrix} 0 & \kappa_g(t) & \kappa_n(t) \\ -\kappa_g(t) & 0 & \tau_g(t) \\ -\kappa_n(t) & -\tau_g(t) & 0 \end{bmatrix} \begin{bmatrix} e(t) \\ h(t) \\ N(t) \end{bmatrix}, \quad (2.1)$$

where $\tau_g(t)$, $\kappa_n(t)$ and $\kappa_g(t)$ are the geodesic torsion, the normal curvature and the geodesic curvature, respectively, of γ at $\gamma(t)$. Since we have so far only considered local geometric entities, the surfaces S and \tilde{S} need not be orientable, i.e. the frame \mathcal{F} and its properties—such as the signs appearing in (2.1)—depend on the local choice of normal vector field N . In the final sections, we will note a few consequences concerning the rolling and the corresponding ribbonization of non-orientable surfaces.

(a) Moving S on \tilde{S}

Given a curve γ on S as above, we now consider smooth and regular curves $\tilde{\gamma}$ on the other surface \tilde{S} such that the following initial compatibility and contact conditions are satisfied:

$$\left. \begin{aligned} \tilde{\gamma}(0) &= \gamma(0) = (0, 0, 0), \\ \tilde{\gamma}'(0) &= \gamma'(0) \\ \|\tilde{\gamma}'\| &= \|\gamma'\|, \end{aligned} \right\} \quad (2.2)$$

and

so that $\tilde{\gamma}$ has the same initial point and direction as γ and so that $\tilde{\gamma}$ has the same speed as γ for all $t \in J$. A framed motion of (S, γ) on \tilde{S} is then defined as follows.

Definition 2.1. Let $E^+(3)$ be the group of direct isometries of \mathbb{R}^3 . A (1-parameter) framed motion g_t of (S, γ) on \tilde{S} along $\tilde{\gamma}$ is a differentiable map $J \rightarrow E^+(3)$ such that for each t the map g_t is the isometry that maps

$$\left. \begin{aligned} \gamma(t) &\text{ to } \tilde{\gamma}(t), \\ \gamma(t) + e(t) &\text{ to } \tilde{\gamma}(t) + \tilde{e}(t) \\ \gamma(t) + N(t) &\text{ to } \tilde{\gamma}(t) + \tilde{N}(t), \end{aligned} \right\} \quad (2.3)$$

and

where \tilde{e} and \tilde{N} are two of the members of the Darboux frame $\tilde{\mathcal{F}} = \{\tilde{e}, \tilde{h} = \tilde{N} \times \tilde{e}, \tilde{N}\}$ along $\tilde{\gamma}$ on \tilde{S} defined in the same way as the frame \mathcal{F} along γ on S . The point $\tilde{\gamma}(t)$ is called the *contact point* at instant t , and $\tilde{\gamma}(J)$ is called the *contact curve* of the framed motion g_t of (S, γ) on \tilde{S} .

Since g_t is in particular an instantaneous isometry it is represented by $x \mapsto R_t x + c_t$, where $R_t \in SO(3)$ is a rotation matrix and c_t is a translation vector. The instantaneous framed motion is then given by the vector field $V_t: x \mapsto \Omega_t(x - c_t) + c'_t$, with $\Omega_t = R'_t R_t^T$ [3]. As g_t is a framed motion we have the following proposition.

Proposition 2.2. Let D_t be the matrix having $e(t)$, $h(t)$ and $N(t)$ as the coordinate column vectors (with respect to a fixed coordinate system in \mathbb{R}^3) and, similarly, let \tilde{D}_t be the matrix having $\tilde{e}(t)$, $\tilde{h}(t)$ and $\tilde{N}(t)$ as the coordinate column vectors (with respect to the same fixed coordinate system in \mathbb{R}^3). Then

$$\left. \begin{aligned} R_t &= \tilde{D}_t D_t^T \\ c_t &= \tilde{\gamma}(t) - R_t \gamma(t), \end{aligned} \right\} \quad (2.4)$$

and

so that

$$g_t(x) = \tilde{D}_t D_t^T (x - \gamma(t)) + \tilde{\gamma}(t). \quad (2.5)$$

Proof. The rotation $\tilde{D}_t D_t^T$ maps the vector $e(t)$ to $\tilde{e}(t)$, and $N(t)$ to $\tilde{N}(t)$. The representation $g_t(x) = R_t x + c_t$ is therefore given by (2.5). ■

(b) Rolling S on \tilde{S}

A framed motion g_t of (S, γ) on \tilde{S} along $\tilde{\gamma}$ is said to be *rotational* if, for all $t \in J$, Ω_t is different from the zero matrix. At each time instant, we can then find a unique vector $\omega_t \neq 0$, the *angular velocity vector*, such that $\omega_t \times x = \Omega_t x$ for all $x \in \mathbb{R}^3$.

Based on the orientation of the angular velocity vector relative to the common tangent plane of $g_t(S)$ and \tilde{S} , we introduce the following terminology for the instantaneous motion—which extends directly to the entire motion.

Definition 2.3. The instantaneous rotational framed motion g_t is called a *pure spinning* if the angular velocity vector ω_t is orthogonal to the tangent plane $T_{\tilde{\gamma}(t)}\tilde{S}$, and a *pure twisting* if ω_t is proportional to the tangent vector $\tilde{e}(t)$. Finally, the motion g_t will be called a *standard rolling* if ω_t does not contain a spinning component and is not a pure twisting, i.e. a standard rolling of S on \tilde{S} is characterized by the condition that there exist smooth functions a and b such that ω_t decomposes as follows for all t :

$$\omega_t = a(t) \cdot \tilde{e}(t) + b(t) \cdot \tilde{h}(t) + 0 \cdot \tilde{N}(t), \quad b(t) \neq 0. \quad (2.6)$$

It turns out that standard rolling of a given surface S on a plane gives a kinematic approach towards the construction of approximating developable ribbons that is presented in §3. To begin with, we observe the following result for the more general situation of rolling S on a general surface \tilde{S} .

Proposition 2.4. *With the setting introduced above, a framed motion g_t of (S, γ) on \tilde{S} along $\tilde{\gamma}$ is a standard rolling if and only if the following conditions are satisfied for all $t \in J$:*

$$\text{and} \quad \left. \begin{aligned} \kappa_g(t) &= \tilde{\kappa}_g(t) \\ \kappa_n(t) &\neq \tilde{\kappa}_n(t), \end{aligned} \right\} \quad (2.7)$$

where $\tilde{\kappa}_g$ and $\tilde{\kappa}_n$ denote the geodesic curvature and the normal curvature of $\tilde{\gamma}$, respectively.

Proof. As in proposition 2.2, $R_t = \tilde{D}_t \tilde{D}_t^T$ and $c_t = \tilde{\gamma}(t) - R_t \gamma(t)$. Then, $g_t(x) = R_t x + c_t$, and so we can find the instantaneous motion V_t by computing $\Omega_t(x - c_t) + c'_t$. Since $c'_t = \tilde{\gamma}'(t) - R'_t \gamma'(t) - R_t \gamma'(t) = -R'_t \gamma'(t)$ for R_t maps $\gamma'(t)$ to $\tilde{\gamma}'(t)$, we obtain

$$\begin{aligned} V_t(x) &= \Omega_t(x - \tilde{\gamma}(t) + R_t \gamma(t)) - R'_t \gamma'(t) \\ &= \Omega_t x - \Omega_t \tilde{\gamma}(t) + R'_t \gamma'(t) - R'_t \gamma'(t) \\ &= \Omega_t(x - \tilde{\gamma}(t)), \end{aligned} \quad (2.8)$$

where $\Omega_t = R'_t R_t^T = \tilde{D}'_t \tilde{D}_t + \tilde{D}_t \tilde{D}_t^T$. If now we let

$$\Lambda_t = \|\gamma'(t)\| \begin{bmatrix} 0 & \kappa_g(t) & \kappa_n(t) \\ -\kappa_g(t) & 0 & \tau_g(t) \\ -\kappa_n(t) & -\tau_g(t) & 0 \end{bmatrix}, \quad (2.9)$$

we have—from (2.1)—that $\tilde{D}'_t = \tilde{D}_t \tilde{\Lambda}_t^T = -\tilde{D}_t \tilde{\Lambda}_t$ ($\tilde{\Lambda}_t$ is skew symmetric) as well as $D_t^T D_t = \Lambda_t$. Hence, if $\Xi_t = \Lambda_t - \tilde{\Lambda}_t$, that is,

$$\Xi_t = \begin{bmatrix} 0 & \Xi_t^{1,2} & \Xi_t^{1,3} \\ -\Xi_t^{1,2} & 0 & \Xi_t^{2,3} \\ -\Xi_t^{1,3} & -\Xi_t^{2,3} & 0 \end{bmatrix}, \quad (2.10)$$

where

$$\left. \begin{aligned} \Xi_t^{1,2} &= \|\gamma'(t)\| \cdot (\kappa_g(t) - \tilde{\kappa}_g(t)), \\ \Xi_t^{1,3} &= \|\gamma'(t)\| \cdot (\kappa_n(t) - \tilde{\kappa}_n(t)), \\ \Xi_t^{2,3} &= \|\gamma'(t)\| \cdot (\tau_g(t) - \tilde{\tau}_g(t)), \end{aligned} \right\} \quad (2.11)$$

and

the expression for Ω_t reduces to

$$\Omega_t = \tilde{D}_t \Xi_t \tilde{D}_t^T, \quad (2.12)$$

and the resulting angular velocity vector of the rolling is thence, with respect to the Darboux frame $\tilde{\mathcal{F}}(t) = \{\tilde{e}(t), \tilde{h}(t), \tilde{N}(t)\}$ along $\tilde{\gamma}$ in \tilde{S} ,

$$\begin{aligned} \omega_t &= (-\Xi_t^{2,3}, \Xi_t^{1,3}, -\Xi_t^{1,2})_{\tilde{\mathcal{F}}(t)} \\ &= \|\gamma'(t)\| \cdot (-\tau_g(t) + \tilde{\tau}_g(t), \kappa_n(t) - \tilde{\kappa}_n(t), -\kappa_g(t) + \tilde{\kappa}_g(t))_{\tilde{\mathcal{F}}(t)}. \end{aligned} \quad (2.13)$$

By comparing (2.13) with (2.6), we see that the conditions (2.7) are necessary and sufficient for g_t to be a standard rolling. ■

In passing we note—for later use—that (2.13) and proposition 2.4 immediately give the coordinates of the pulled-back angular rotation vector $\hat{\omega}_t = R_t^T \omega_t$ with respect to the frame $\mathcal{F}(t)$ for a standard rolling

$$\hat{\omega}_t = \|\gamma'(t)\| \cdot (-\tau_g(t) + \tilde{\tau}_g(t), \kappa_n(t) - \tilde{\kappa}_n(t), 0)_{\mathcal{F}(t)}. \quad (2.14)$$

The important special case in which \tilde{S} is a plane is covered by the following corollary.

Corollary 2.5. *If \tilde{S} is a plane, then the motion g_t is a standard rolling if and only if*

$$\text{and} \quad \left. \begin{aligned} \kappa_g(t) &= \tilde{\kappa}_g(t) \\ \kappa_n(t) &\neq 0. \end{aligned} \right\} \quad (2.15)$$

The instantaneous angular rotation vector ω_t and its pull-back $\hat{\omega}_t$ are correspondingly, in $\tilde{\mathcal{F}}(t)$ and $\mathcal{F}(t)$, respectively

$$\begin{aligned} \omega_t &= \|\gamma'(t)\| \cdot (-\tau_g(t), \kappa_n(t), 0)_{\tilde{\mathcal{F}}(t)} \\ &= \|\gamma'(t)\| \cdot (-\tau_g(t), \kappa_n(t), 0)_{\mathcal{F}(t)}, \end{aligned} \quad (2.16)$$

where now $\tilde{\mathcal{F}}(t) = \{\tilde{e}(t), \tilde{e}_3 \times \tilde{e}(t), \tilde{e}_3\}$ is the co-moving frame in the plane with constant normal vector field \tilde{e}_3 along $\tilde{\gamma}$.

3. Developable Cartan surface ribbons

In this section, we show that the rolling discussed above serves as a tool for obtaining a flat developable approximation of the surface S along γ . This is an alternative to constructing developable approximations via envelopes of tangent planes along γ [20, pp. 195–197]. In [9], osculating developable surfaces and their singularities have been studied; see also [21]. It will follow from the condition (2.15) that the approximating surface is free of singularities in a neighbourhood of γ ; see theorem 3.1.

We first consider the notion of ruled surfaces, since developable surfaces constitute a special subcategory of these.

Let w_- and w_+ denote two positive functions on the given t -interval J , let $I = [-w_-(t), w_+(t)]$, and let V denote the corresponding parameter domain in \mathbb{R}^2 . A parametrized ruled surface (with boundary) $r: V \rightarrow \mathbb{R}^3$ based on the centre curve γ is determined by a non-vanishing vector field β along γ

$$r(t, u) = \gamma(t) + u \cdot \beta(t), \quad t \in J, u \in I. \quad (3.1)$$

We will assume that β is a unit vector field along γ and that the surface r is regular, i.e. its partial derivatives are linearly independent for all u in the interval $[-w_-(t), w_+(t)]$, $t \in J$. Regularity implies in particular that

$$\beta(t) \neq \pm e(t) \quad \text{for all } t \in J. \quad (3.2)$$

Moreover, the surface $r(V)$ is flat (with Gaussian curvature zero at all points, i.e. developable), precisely when the following condition is satisfied [20, p. 194]:

$$\beta' \cdot (\beta \times e) = 0. \quad (3.3)$$

If $r(V)$ is eventually to be constructed so that it becomes a flat approximation of S along γ , we need to find a regular parametrization r such that $r(V)$ is developable and has the same normal field N as S along γ . This means that we need to determine the vector function β so that it fulfils (3.2), (3.3) and

$$\beta \cdot N = 0. \quad (3.4)$$

The desired vector function β is precisely (modulo length and sign) the previously encountered pulled-back angular velocity vector $\hat{\omega}_t$ along γ associated with the rolling of S along $\tilde{\gamma}$ on a plane [10].

Theorem 3.1. *Let γ denote a smooth curve on a surface S and let $\mathcal{F} = \{e, h, N\}$ be the corresponding Darboux frame field along γ . Suppose that the normal curvature function κ_n for γ on S never vanishes.*

Then there exists a unique developable surface which contains γ and which has everywhere the same tangent plane as S along γ . It is parametrized as follows:

$$r(t, u) = \gamma(t) + u \cdot \frac{\hat{\omega}_t}{\|\hat{\omega}_t\|}, \quad u \in [w_-(t), w_+(t)], \quad t \in J, \quad (3.5)$$

where $\hat{\omega}_t$ denotes the pulled-back angular velocity vector

$$\left. \begin{aligned} \hat{\omega}_t &= \kappa_n(t) \cdot h(t) - \tau_g(t) \cdot e(t) \\ \|\hat{\omega}_t\| &= \sqrt{\kappa_n^2(t) + \tau_g^2(t)}. \end{aligned} \right\} \quad (3.6)$$

and

Proof. Write β in terms of its coordinate functions $\beta \cdot e$ and $\beta \cdot h$, substitute into equation (3.3) and apply equation (2.1) to express the derivatives of e and h . Then

$$\frac{\beta \cdot e}{\beta \cdot h} = -\frac{\tau_g}{\kappa_n}, \quad (3.7)$$

and the result follows upon normalization of the solution β . The ruling directions of the developable surface are thus given by the instantaneous angular velocity vector of the rolling. ■

Definition 3.2. The developable surface, which is parametrized by (3.5)—and which is therefore approximating the surface S —will be called the *Cartan surface ribbon* along γ on S .

As is already in the name, the Cartan surface ribbon can be *developed* isometrically into a planar ribbon.

Definition 3.3. The *associated Cartan planar ribbon* for γ on S —which is defined along $\tilde{\gamma}$ in the plane—is now determined via (3.8) in proposition 3.4, which also establishes the isometry between the two Cartan ribbons.

Proposition 3.4. An isometry from the Cartan surface ribbon onto the associated Cartan planar ribbon is realized along the development curve $\tilde{\gamma}$ in the following way, which is in precise accordance with the previously found rolling of S along γ on the plane with contact curve $\tilde{\gamma}$. We simply map the point $r(t, u)$ to the point

$$\begin{aligned} \tilde{r}(t, u) &= \tilde{\gamma}(t) + u \cdot \frac{\omega_t}{\|\omega_t\|} \\ &= \tilde{\gamma}(t) + u \cdot \frac{\omega_t}{\sqrt{\kappa_n^2(t) + \tau_g^2(t)}}. \end{aligned} \quad (3.8)$$

Proof. We let $\beta(t) = \omega_t / \|\omega_t\|$ and $\hat{\beta}(t) = \hat{\omega}_t / \|\hat{\omega}_t\|$. Since $\kappa_g(t) = \tilde{\kappa}_g(t)$ all the scalar products between two vectors chosen from $\{\gamma'(t), \hat{\beta}(t), \hat{\beta}'(t)\}$ are the same as the scalar products between the corresponding two vectors chosen from $\{\tilde{\gamma}'(t), \beta(t), \beta'(t)\}$. It follows that the two first fundamental forms for $r(t, u)$ and $\tilde{r}(t, u)$, respectively, have identical coordinate functions. The two ribbons r and \tilde{r} are therefore isometric. ■

Remark 3.5. In all of the above constructions, we have assumed that the centre curves in question have nowhere vanishing normal curvature. For a number of cases, the normal curvature does vanish, such as on planar faces of polyhedra and through lines of inflections on generalized cylindrical faces. The method of approximation by ribbons can be extended to these surfaces by cut and paste along the singular rulings under the condition that the geodesic torsion also vanishes together with the normal curvature. For example, for surfaces containing planar domains, the ribbonization can be continued over any edge of the planar domain if the ruling of the ribbon agrees with the given edge. For polyhedral surfaces, this is always possible. A ribbon with planar patches will also be denoted a Cartan ribbon; see the later section on Euler's polyhedral formula.

(a) Curvature and parallel transport

In view of our observations concerning the rolling of S on the plane, it now makes sense to say that the Cartan surface ribbon can be *rolled* isometrically onto the associated Cartan planar ribbon. This is induced in the way just described by the rolling of S on the plane, which itself is represented by the pulled-back angular velocity vector field $\hat{\omega}$ along γ in S and by ω along $\tilde{\gamma}$ in the plane. Accordingly, once the centre curve $\tilde{\gamma}$ in the plane has been constructed using $\tilde{\kappa}_g(t) = \kappa_g(t)$, then the approximating Cartan *surface* ribbon can be obtained via the inverse rolling of the Cartan *planar* ribbon backwards into contact with the surface S along γ . An early hint of this connection is presented in [22, pp. 227–228].

The key object for the actual construction of the approximating Cartan surface ribbon along a given curve γ on S is thence the planar curve $\tilde{\gamma}$, which may itself be constructed either by rolling or—more simply—by integrating the curvature function κ_g of γ , but in the plane, in the well-known way [20].

Proposition 3.6. *Suppose $\tilde{\gamma}$ has (signed) curvature κ_g and speed $\|\tilde{\gamma}'\| = v$. Then, modulo rotation and translation in the plane, we have*

$$\tilde{\gamma}(t) = \int_0^t v(\hat{t}) \cdot (\cos(\varphi(\hat{t})), \sin(\varphi(\hat{t}))) \, d\hat{t}, \quad (3.9)$$

where

$$\varphi(\hat{t}) = \int_0^{\hat{t}} v(\hat{u}) \cdot \kappa_g(\hat{u}) \, d\hat{u}. \quad (3.10)$$

The curve $\tilde{\gamma}$ appears as a special—and simple—example of a *Cartan development* as already alluded to via the reference to Nomizu's initial work [3]. This is why the ensuing developable ribbons are called *Cartan surface ribbons*. To be a bit more specific concerning our simple two-dimensional setting, we recall in particular the important geodesic curvature equivalence used above.

We let the tangent space $T_{\gamma(0)}S$ at $\gamma(0)$ represent the plane \tilde{S} into which we want to construct the Cartan development curve corresponding to the given curve γ in S . For each t , we consider the parallel transport of the tangent vector $\gamma'(t)$ along γ from the point $\gamma(t)$ to the point $\gamma(0)$ [4, p. 131],

$$X(t) = \Pi_{\gamma}^{\gamma(t), \gamma(0)}(\gamma'(t)). \quad (3.11)$$

The Cartan development $\tilde{\gamma}$ of γ in $T_{\gamma(0)}S$ is then

$$\tilde{\gamma}(t) = \int_0^t X(u) \, du. \quad (3.12)$$

From this construction, we have, in particular, the following.

Proposition 3.7. *Any tangent vector $\tilde{\gamma}'(t_1) = X(t_1)$ is itself parallelly transported (in the usual Euclidean sense) along $\tilde{\gamma}$ in the tangent space $T_{\gamma(0)}S$ (which may be canonically identified with $T_{\tilde{\gamma}(0)}\tilde{S}$) from $(0,0)$ to $\tilde{\gamma}(t_1)$ and the (geodesic) curvature function of the planar curve $\tilde{\gamma}$ is equal to the geodesic curvature function of the original curve γ in S ,*

$$\tilde{\kappa}_g(t) = \kappa_g(t) \quad \text{for all } t. \quad (3.13)$$

Proof. Suppose Y is any parallel vector field along the curve γ on the surface S , then the angle $\theta(t) = \angle(Y(t), \gamma'(t))$ gives the geodesic curvature of γ via $\theta'(t) = \kappa_g(t)$. Since the same holds true by construction along the development curve $\tilde{\gamma}$ in the tangent plane, we get $\tilde{\theta}(t) = \theta(t)$, so that $\tilde{\kappa}_g = \kappa_g$. ■

(b) A measure of local goodness of Cartan ribbon approximations

A measure of the goodness of a single ribbon approximation along a given centre curve γ can be obtained from the following construction. Close to γ the surface S can be parametrized as a graph

surface ‘over’ the Cartan ribbon in the direction of the normal field N of the ribbon as follows:

$$S_\varepsilon : \sigma(t, u) = \gamma(t) + u \cdot \left(\frac{\kappa_n(t)h(t) - \tau_g(t)e(t)}{\sqrt{\kappa_n^2(t) + \tau_g^2(t)}} \right) + f(t, u) \cdot N(t), \quad t \in J \text{ and } u \in [-\varepsilon, \varepsilon], \quad (3.14)$$

where f denotes the corresponding ‘height’ function and ε is everywhere smaller than each of the width functions w_- and w_+ for all $t \in J$ along γ . (Both width functions have positive minima since they are positive and J is closed.) The function f clearly has $f(t, 0) = f'(t, 0) = 0$ for all $t \in J$, so that

$$f(t, u) = \frac{1}{2}f''(t, 0) \cdot u^2 + O(u^3) \quad \text{for each } t \in J \text{ and for all } u \in [-\varepsilon, \varepsilon]. \quad (3.15)$$

The domain in space that is enclosed ‘between’ the surface S_ε and the Cartan ribbon is thence parametrized as follows:

$$\mathcal{D}_\varepsilon : R(t, u, w) = \gamma(t) + u \cdot \left(\frac{\kappa_n(t)h(t) - \tau_g(t)e(t)}{\sqrt{\kappa_n^2(t) + \tau_g^2(t)}} \right) + w \cdot f(t, u) \cdot N(t),$$

where $t \in J$, $u \in [-\varepsilon, \varepsilon]$, $w \in [0, 1]$. (3.16)

Definition 3.8. We consider the volume of the domain \mathcal{D}_ε as a natural local measure of goodness $\mathcal{M}(\gamma, \varepsilon)$ of our approximation of the surface S , i.e. of the approximation by the single Cartan ribbon to S_ε along the centre curve γ ,

$$\mathcal{M}(\gamma, \varepsilon) = \text{Vol}(\mathcal{D}_\varepsilon) = \int_J \int_{-\varepsilon}^{\varepsilon} \int_0^1 |(R'_t \times R'_u) \cdot R'_w| \, dt \, du \, dw. \quad (3.17)$$

We then have the following evaluation for the volume of \mathcal{D}_ε .

Theorem 3.9. The goodness $\mathcal{M}(\gamma, \varepsilon)$ of the single ribbon approximation along a unit speed centre curve γ can be expressed in terms of the curvature functions $H(t)$, $K(t)$, $\kappa_n(t)$ and $\tau_g(t)$ along γ as follows:

$$\mathcal{M}(\gamma, \varepsilon) = \frac{1}{3}\varepsilon^3 \cdot \int_J F(H(t), K(t), \kappa_n(t), \tau_g(t)) \, dt + O(\varepsilon^4), \quad (3.18)$$

where

$$F(H, K, \kappa_n, \tau_g) = \frac{\kappa_n^2}{(\kappa_n^2 + \tau_g^2)^{3/2}} \cdot \left| \left(\tau_g^2 - \kappa_n^2 + 2H\kappa_n - 2\tau_g \sqrt{2H\kappa_n - K - \kappa_n^2} \right) \right|. \quad (3.19)$$

Proof. Using the parametrization of \mathcal{D}_ε and the derivatives of the Darboux frame in (2.1), we find that the volume element $|(R'_t \times R'_u) \cdot R'_w|$ has the following leading term:

$$|(R'_t \times R'_u) \cdot R'_w| = \left| \frac{1}{2}f''_{uu}(t, 0) \cdot \frac{u^2 \cdot \kappa_n(t)}{\sqrt{\kappa_n^2(t) + \tau_g^2(t)}} \right| + O(u^3). \quad (3.20)$$

The second derivative $f''_{uu}(t, 0)$ is precisely the normal curvature of the surface S in the direction of the ruling line of the Cartan ribbon at $\gamma(t)$. It can thence be expressed by the curvature function values $H(t)$, $K(t)$, $\kappa_n(t)$ and $\tau_g(t)$ at $\gamma(t)$ along γ ,

$$f''_{uu}(t, 0) = \frac{\kappa_n}{\kappa_n^2 + \tau_g^2} (\tau_g^2 - \kappa_n^2 + 2H\kappa_n - 2\tau_g \sqrt{2H\kappa_n - K - \kappa_n^2}). \quad (3.21)$$

Insertion into (3.20) then gives

$$\begin{aligned}
 \mathcal{M}(\gamma, \varepsilon) &= \int_J \int_{-\varepsilon}^{\varepsilon} \int_0^1 |(R'_t \times R'_u) \cdot R'_w| \, dt \, du \, dw \\
 &= \int_J \int_{-\varepsilon}^{\varepsilon} \left| \frac{1}{2} \cdot \frac{u^2 \cdot \kappa_n^2}{(\kappa_n^2 + \tau_g^2)^{3/2}} (\tau_g^2 - \kappa_n^2 + 2H\kappa_n - 2\tau_g \sqrt{2H\kappa_n - K - \kappa_n^2}) \right| + O(u^3) \, dt \, du \\
 &= \frac{1}{3} \varepsilon^3 \cdot \int_J \left| \frac{\kappa_n^2}{(\kappa_n^2 + \tau_g^2)^{3/2}} (\tau_g^2 - \kappa_n^2 + 2H\kappa_n - 2\tau_g \sqrt{2H\kappa_n - K - \kappa_n^2}) \right| dt + O(\varepsilon^4) \\
 &= \frac{1}{3} \varepsilon^3 \cdot \int_J F(H(t), K(t), \kappa_n(t), \tau_g(t)) \, dt + O(\varepsilon^4). \quad \blacksquare
 \end{aligned}$$

Corollary 3.10. Suppose that the centre curve γ is a line of curvature on the surface S —as is the case for all the chosen centre curves on the ellipsoid considered in §6. Then the geodesic torsion of γ vanishes identically and the corresponding local measure of goodness of the Cartan ribbon along γ reduces to

$$\mathcal{M}(\gamma, \varepsilon) = \frac{1}{3} \varepsilon^3 \cdot \int_J |\kappa_n(h(t))| \, dt + O(\varepsilon^4), \quad (3.22)$$

where $\kappa_n(h(t))$ denotes the normal curvature of S at $\gamma(t)$ in the direction of $h(t)$, which is orthogonal to $\gamma'(t)$.

Proof. This follows directly from equation (3.20) and the fact that in this case we have $f''_{uu}(t, 0) = \kappa_n(h(t))$. ■

Another consequence of theorem 3.9 is the following result, which is not surprising, since we are approximating the surface S with flat Cartan ribbons.

Corollary 3.11. Suppose that the Gaussian curvature K of S vanishes identically along γ . Then

$$\mathcal{M}(\gamma, \varepsilon) = O(\varepsilon^4). \quad (3.23)$$

Proof. This follows readily by inserting the following ingredients into the formula (3.18):

$$K(t) = 0; \quad H(t) = \kappa_1(t); \quad \kappa_2(t) = 0; \quad \tau_g(t) = \kappa_1(t) \cos(\theta(t)) \sin(\theta(t)); \quad \kappa_n(t) = \kappa_1(t) \cos^2(\theta(t)),$$

where $\theta(t)$ denotes the angle between $\gamma'(t)$ and the principal direction of curvature for S at $\gamma(t)$ corresponding to the principal curvature $\kappa_1(t)$. ■

Remark 3.12. Although theorem 3.9 is but an initial step towards a global measure of goodness for the total number of individual Cartan ribbons (which are in use for the overall approximation of a given full surface), it may still be possible and reasonable to apply the formula (3.18)—or a proper refinement of it—for each ribbon and then simply sum the values of goodness over the number of ribbons. Naturally, the u -domain of integration should then not just be $[-\varepsilon, \varepsilon]$ but rather the full-width interval $[-w_-(t), w_+(t)]$ along the respective ribbons. Moreover, good single ribbon approximations (and their higher dimensional analogues) represent an interesting alternative basis and tool for principal geodesic analysis, and for polynomial regression in general, on surfaces and in Riemannian manifolds [23,24]. In particular, in that setting the notion of Riemannian polynomials has also been studied via rolling maps [25,26]—much in the same vein as we have employed the concept of rolling in the present work.

(c) The local cut-off procedure for neighbouring ribbons

We consider two neighbouring centre curves γ^1 and γ^2 for two neighbouring Cartan ribbons and prove the existence of their intersection curve, which eventually constitutes the wedge (or cut-off) curve in space ‘between’ the two centre curves; see the examples in §§5 and 6. The wedge thereby defines the actual width functions w_-^2 and w_+^1 that are used for the final ribbonization of the surface S . In this setting, w_+^1 is to be thought of as the cut-off function for γ^1 in the direction towards γ^2 , and w_-^2 is the cut-off function for γ^2 in the (opposite) direction from γ^2 towards γ^1 .

Proposition 3.13. *The wedges are well defined for each pair of neighbouring Cartan ribbons, i.e. the cut-off functions exist, provided the corresponding centre curves are pairwise sufficiently close to each other.*

Proof. We sketch the proof as follows. Suppose that r_1 is the ruling line at some point p on γ^1 . We must show that (for close-by neighbouring centre curves) there is a corresponding ruling line r_2 at some point of γ^2 so that the two rulings intersect in a (cut-off) point, i.e. so that w_+^1 and w_-^2 exist. Obviously, this does not necessarily work for centre curves that are far apart from each other, so we need to assume that the centre curves are sufficiently close.

We may also assume that the two centre curves are neighbouring coordinate curves in a special local parametrization of a tubular neighbourhood on S around γ^1 . Specifically, without lack of generality, we parametrize the neighbourhood by a smooth vector function ρ with parameters t and v such that the following properties are satisfied: $\rho(t, 0) = \gamma^1(t)$; $\rho(t, \varepsilon) = \gamma^2(t)$; every t -coordinate curve has non-vanishing normal curvature: $\kappa_n(\rho'_t(t, v)) \neq 0$; and $\rho'_v(t_0, v)$ is in the direction of the ruling line of the Cartan ribbon along the curve $\rho(t, v)$ at the point $\rho(t_0, v)$ for all $v \in [0, \varepsilon]$.

This latter condition means that the curve $q_{t_0}(v) = \rho(t_0, v)$, $v \in [0, \varepsilon]$, has tangent lines that are ruling lines of the respective Cartan ribbons along the centre curves $\rho(t, v)$ for each v in the said interval.

If the curve q_{t_0} has non-zero curvature at $v = 0$ (and possibly also nonzero torsion there), then an intersection argument in the ambient space shows that there exists a ruling line of the Cartan ribbon at some point $\rho(t_2, \varepsilon)$ along the centre curve $\rho(t, \varepsilon)$ close to $\rho(t_0, \varepsilon)$, i.e. for t_2 close to t_0 , which intersects the ruling line r_1 based at $p = \rho(t_0, 0)$ —provided ε is sufficiently small. If the torsion of the curve q_{t_0} vanishes in the interval $v \in [0, \varepsilon]$ so that it is planar in that interval, then $t_2 = t_0$ and the intersection takes place in that plane.

The same argument holds if q_{t_0} has zero curvature at $v = 0$ but, say, has positive curvature for $v \in]\delta, \varepsilon]$. Moreover, if q_{t_0} has zero curvature in an interval, $v \in [0, \varepsilon]$, then q_{t_0} is a straight line in that interval and every point on the ruler from p is also a point on a ruler for the ribbon with centre curve $\eta(t, v_0)$ for any v_0 in that interval, and the corresponding cut-off value for w_+^1 can be chosen to be any value in $]0, \varepsilon]$. ■

4. Gauss–Bonnet inspection

We consider a finite (piecewise smooth) ribbonization $\mathcal{R} = \cup_i^R \mathcal{R}_i$, $R = \#\mathcal{R}$, of S , all of whose Cartan surface ribbons \mathcal{R}_i , $i = 1, \dots, R$, are closed in the sense that they are based on closed smooth centre curves on S , as exemplified in §5. Let $\mathcal{W} = \cup_i \mathcal{W}_i$ denote the system of (piecewise smooth) wedge curves stemming from the ribbonization \mathcal{R} and let $\hat{\mathcal{W}}$ denote the corresponding planar wedge curve system of the Cartan planar ribbons $\hat{\mathcal{R}}$. The end (cut-)curves of the planar ribbons—which are typically needed in order to obtain the planar representation of the ribbons—are not considered part of $\hat{\mathcal{W}}$.

We now apply the Gauss–Bonnet theorem to surfaces which are ribbonized by such circular ribbons.

The system of wedge curves \mathcal{W} consists of curves with possible branch points, where three or more ribbons come together, and with possible endpoints, where one ribbon is locally bent around the wedge (and is thus in contact with itself), as in the top and bottom ribbon on the ellipsoid, as exemplified in §6.

We may assume without lack of generality that the branch points and endpoints are all isolated and regular in the sense that the wedge curves in a neighbourhood of such points can be mapped diffeomorphically to a corresponding star configuration in \mathbb{R}^3 with a number of straight line segments issuing from a common vertex. The branch points and endpoints are called *vertices* of the ribbonization \mathcal{R} . The vertex set is denoted by \mathcal{P} and the number of vertices by $P = \#\mathcal{P}$. The number of segments issuing from a given vertex p_k in the vertex set \mathcal{P} is called the *degree*, $d_k = d(p_k)$, of the vertex. If a ribbon has an isolated cone point then this is also a vertex, and—in accordance with the above definition—we count its degree as 0.

Theorem 4.1. *The Euler characteristic, $\chi(\mathcal{R})$, of a ribbonization \mathcal{R} is*

$$\chi(\mathcal{R}) = \frac{1}{2} \sum_{k=1}^P (2 - d_k). \quad (4.1)$$

Proof. The total curvature contributions for the Gauss–Bonnet theorem can be divided into three parts:

(a) *Surface contributions:* the surface integral of the Gauss curvature K ,

$$C_{\mathcal{R} \setminus \mathcal{W} \cup \mathcal{P}} = \int_{\mathcal{R} \setminus \mathcal{W} \cup \mathcal{P}} K \, d\mu = 0. \quad (4.2)$$

(b) *Wedge contributions:* the integral of the geodesic curvature along the edges of the Cartan ribbons excluding the vertex points,

$$C_{\mathcal{W} \setminus \mathcal{P}} = \sum_{q=1}^R \int_{\mathcal{W}_q \setminus \mathcal{P}_q} \kappa^{\mathcal{W}_q}(s) \, ds. \quad (4.3)$$

(c) *Vertex contributions:* sum of the angular deficit (angular defect) at the vertices, i.e. 2π minus the sum of the inner angles $\beta(j, k)$ at the vertices. The inner angles are replaced by the corresponding outer angles $\alpha(j, k)$ as $\alpha = \pi - \beta$, where $\alpha \in [-\pi, \pi]$ and $\beta \in [0, 2\pi]$,

$$\begin{aligned} C_{\mathcal{P}} &= \sum_{j=1}^P \left(2\pi - \sum_{k=1}^{d_k} \beta(j, k) \right) \\ &= \sum_{k=1}^P \left(2\pi - \sum_{j=1}^{d_k} (\pi - \alpha(j, k)) \right) \\ &= \sum_{k=1}^P (2\pi - \pi d_k) + \sum_{k=1}^P \sum_{j=1}^{d_k} \alpha(j, k). \end{aligned} \quad (4.4)$$

Summarizing: adding these contributions together, we find

$$2\pi \cdot \chi(\mathcal{R}) = \sum_{q=1}^R \int_{\mathcal{W}_q \setminus \mathcal{P}_q} \kappa^{\mathcal{W}_q}(s) \, ds + \sum_{k=1}^P \sum_{j=1}^{d_k} \alpha(j, k) + \sum_{k=1}^P (2\pi - \pi d_k). \quad (4.5)$$

By a permutation of the outer angles in the second term, one can group them according to the ribbon wedge curves they appear on. This is possible because each of the kinks on the ribbons is encountered precisely once in the summation. Further, as the ribbons are closed it follows that their wedge integral and the corresponding sum of outer angles together cancel to zero. Hence one is left with the equality

$$\chi = \frac{1}{2} \sum_{k=1}^P (2 - d_k). \quad (4.6)$$

■

Remark 4.2. As already mentioned, the set of vertices, \mathcal{P} , is a feature of the three-dimensional mesh of wedge curves. Wedge curves from two, most commonly distinct, ribbons follow each other until a vertex point, where, for example, three ribbons come together. We summarize the different vertex characters in [table 1](#).

The ribbon formula in theorem 4.1 is valid for orientable as well as non-orientable surfaces. To see this, we only need to show that the formula does not change whether the ribbons are regular closed ribbons or Möbius strip ribbons. This follows as a consequence of lemma 4.3.

Table 1. A characterization of vertices.

| d_k | vertex character | classification |
|-------|-----------------------------------|--------------------------|
| 0 | fully circumscribed by one ribbon | cone point |
| 1 | half circumscribed by a ribbon | wedge endpoint |
| 2 | two ribbons meet at the point | zero contributing vertex |
| >2 | $n > 2$ ribbons meet | conventional vertex |

Lemma 4.3. *A conventional cylindrical closed ribbon (without vertices) and a Möbius strip ribbon both contribute zero to the total curvature integral.*

Proof. It follows simply by cutting the ribbons along a ruler. In this case, the ribbons can be fully flattened and have a total curvature contribution of 2π , which is equal to the sum of the four artificial angles introduced by the cutting along the ruler. The difference between a ribbon that is orientable and one that is not consists of a simple permutation of the four inner angles of the cut. ■

For the explicit extension of theorem 4.1 to Cartan ribbonizations that include ribbons with open centre curves, it is sufficient to count the number N_O of such ribbons, and equation (4.1) becomes

$$\chi = \frac{1}{2} \sum_{k=1}^P (2 - d_k) + N_O. \quad (4.7)$$

Remark 4.4. A necessary and sufficient criterion for the correct representation of the topology of the surface S by a given ribbonization is the following. For each ribbon, there exists a homeomorphism which maps the ribbon to a domain on the surface such that

- (i) the contact structure (edges and vertices) between the individual ribbons is preserved
- (ii) the full surface S is covered precisely once by the images of the ribbons.

For ribbonizations with sufficiently narrow ribbons, i.e. with small cut-off functions w_- and w_+ , such homeomorphisms can for example be obtained via normal projection (along the orthogonal lines to S) of the ribbons into the surface.

(a) From ribbon inspection to the Euler polyhedral formula

We consider a polyhedron Q and apply the conventional notation, i.e. F , E and V denote the number of faces, of edges and of vertices, respectively, of the *polyhedron*. To apply the ribbon formula (4.1), we need to cover the polyhedron with closed ribbons. One can cover each one of the F faces by a closed ribbon with a (flat) vertex covering the intrinsic part of the face polygon. With this choice, there are then F new such virtual vertices, all with degree zero. We therefore have the total number of ribbon vertices

$$P = V + F \quad (4.8)$$

and

$$\sum_{k=1}^P d_k = 2 \cdot E. \quad (4.9)$$

Hence we recover the well-known polyhedron formula from the ribbon formula,

$$\chi(Q) = \frac{1}{2} \sum_{k=1}^P (2 - d_k) = \frac{2(V + F) - 2E}{2} = V - E + F. \quad (4.10)$$

5. An unknot-based Cartan ribbonized torus

This example is concerned with the ribbonization of the torus

$$\mathcal{T}^2: \sigma(u, v) = ((2 + \cos(u)) \cdot \cos(v), (2 + \cos(u)) \cdot \sin(v), \sin(u)), \quad (u, v) \in \mathbb{R}^2 \quad (5.1)$$

using the following two closed curves as the centre curves (figure 1a):

$$\left. \begin{aligned} \gamma_1(t) &= \sigma(3 \cdot t, t), \quad t \in [-\pi, \pi], \\ \gamma_2(t) &= \sigma\left(3 \cdot t, t + \frac{\pi}{3}\right), \quad t \in [-\pi, \pi]. \end{aligned} \right\} \quad (5.2)$$

The corresponding two Cartan surface ribbons are then constructed (with constant and equal width functions) along the two curves, using the parametrization recipe in (3.5). They are displayed in figure 1b. The ribbons are then widened in \mathbb{R}^3 in the direction of $\pm\omega$ until intersection with their respective neighbour ribbons; see §3c.

In the present example, the planar ribbons are constructed via the planar centre curves $\tilde{\gamma}$ from (3.9) using the geodesic curvature function from the curves (5.2) on the torus.

The intersection width functions are obtained numerically by solving the intersection equation for each value of t along the centre curves (figure 2). Once the cut-off widths w_{\pm} of the Cartan surface ribbons have been determined, the corresponding Cartan planar ribbons (with the same width functions $w_{\pm}(t)$) are finally constructed from the planar centre curve with the same geodesic curvature as the original centre curve on the surface. In this particular case, both Cartan planar ribbons are identical—one of them is displayed in figure 3.

(a) Inspection of the ribbonized torus

The number of vertices of the above ribbonization is 0 and, hence, according to equation (4.6), we immediately get the Euler characteristic $\chi = 0$ for the torus.

6. Curvature line-based ribbonizations of an ellipsoid

A curvature line parametrization of the ellipsoid with half axes $\sqrt{a} > \sqrt{b} > \sqrt{c} > 0$ is obtained as follows [8, example 7.4; 27]:

$$\sigma(u, v) = \left(\pm \sqrt{\frac{a(a-u)(a-v)}{(a-b)(a-c)}}, \pm \sqrt{\frac{b(b-u)(b-v)}{(b-a)(b-c)}}, \pm \sqrt{\frac{c(c-u)(c-v)}{(c-a)(c-b)}} \right), \quad (6.1)$$

where $u \in (b, a)$ and $v \in (c, b)$. This particular parametrization of the ellipsoid is shown in the leftmost display in figure 4. As shown in figure 4 the coordinate (curvature) lines of this parametrization extend smoothly from one octant to a neighbouring octant except at the four umbilical points on the ellipsoid corresponding to parameter values $u \rightarrow b$ and $v \rightarrow b$.

Such curvature line ribbonizations are interesting, partly because they give non-trivial illustrations of the simple measure of goodness established in corollary 3.10, and partly because they also clearly highlight the significant umbilical points. The umbilics on the ellipsoid considered here correspond to the four endpoints of the wedge segments that appear on the top cap and on the bottom cap—both visible in the second display from the left in figure 4.

(a) Inspection of the ellipsoid

The ellipsoid has four vertices—corresponding to the four umbilical points—each of degree 1, $d_k = 1$, and each therefore contributing one-half to the Euler characteristic; see equation (4.1).

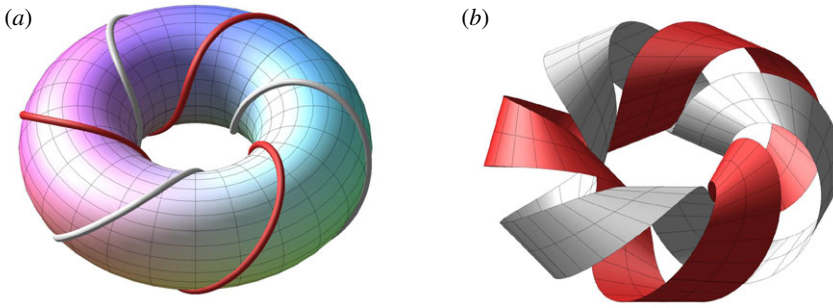


Figure 1. (a) Two $(3,1)$ -unknots on a torus. (b) They are used as centre curves for the beginning of a Cartan ribbonization of the torus. See figure 2 with the corresponding ribbons, extended and cut-off. (Online version in colour.)

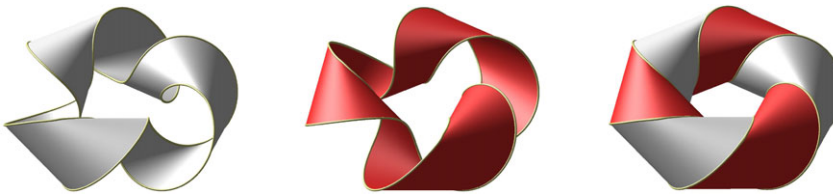


Figure 2. Ribbonization of the torus along two $(3, 1)$ -unknots with the correct cut-off width functions. (Online version in colour.)



Figure 3. The geometry of one of the two identical planar ribbons used for the covering of the torus in figure 2. (Online version in colour.)

7. Comparison with classical topological inspections

As illustrated above, the topology of the surface can be read off from a ribbonization—in fact often in an easier way than from a triangulation. In this section, we will briefly compare the above inspection with the methods of Morse and Poincaré–Hopf based on inspections of Morse height functions and their corresponding vector fields, respectively.

Consider a Morse height function f on a surface S and choose centre curves for a ribbonization among level curves of f . Since the saddle points of f are isolated the centre curves can be chosen to be arbitrarily close and yet with tangents avoiding asymptotic directions, so that such ribbonizations exist and have the same topology as the surface. Moreover, as a third perspective, the gradient of f on S represents a vector field whose indices also count its topology.

Based on a Morse height function these three topological inspections are all based on countings of minima, maxima and saddle points. Clearly, the final summations give the same result when applying table 2.

In the case of a torus with its classical Morse height function [30, diagram 1 p. 1], the corresponding ribbonizations all have one minimum, one maximum (both with degree $d_k = 0$) and two saddle points (with degrees $d_k = 4$), so that the sum is $\frac{1}{2} \sum_{k=1}^{n_v} (2 - d_k) = 0$, as expected. An interesting Morse height function for the non-orientable Boy's model of $\mathbb{R}P^2$ in \mathbb{R}^3 , which may likewise be used as centre curves for a ribbonization, is presented by U. Pinkall in [31, ch. 6,

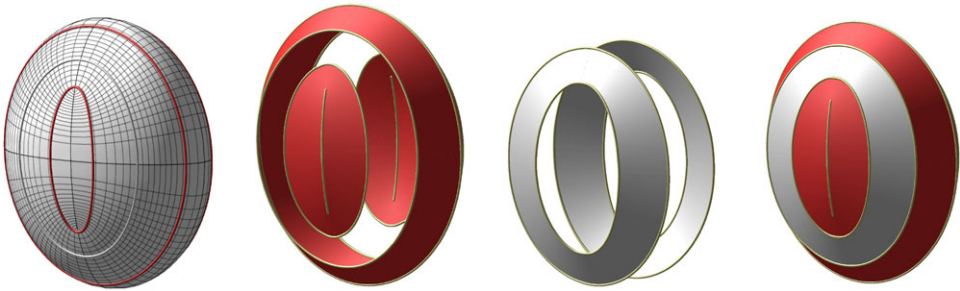


Figure 4. Ribbonization of the ellipsoid with half axes $\sqrt{5}, 2$ and 1 corresponding to the parameters $(a, b, c) = (5, 4, 1)$ in the representation (6.1). The ribbonization is built from six Cartan surface ribbons along the indicated line-of-curvature centre lines, which intersect the horizontal ‘equator’ at equi-distributed points. (Online version in colour.)

Table 2. Listing the relationship between degrees of vertices, d_k , Morse indices, γ , and the indices, l , of a vector field for smooth two-dimensional manifolds. Also compared are the corresponding three topological inspections for the Euler characteristic: the ribbon inspection, based on vertex counting; the Morse index formula, based on critical points of Morse functions [28]; and the Poincaré–Hopf formula, based on the counting of types of zeros of a vector field [29].

| | ribbon (d_k) | Morse (γ) | vector field (l) |
|--------------|--|---|------------------------|
| minimum | 0 | 0 | 1 |
| saddle point | 4 | 1 | −1 |
| maximum | 0 | 2 | 1 |
| χ | $\frac{1}{2} \sum_{k=1}^{n_v} (2 - d_k)$ | $\sum_{\gamma=0}^{\gamma=2} (-1)^\gamma n_\gamma$ | $\sum_{k=1}^{n_z} l_k$ |

pp. 63–67, figs 6.7 and 6.8]. This particular ribbonization has four vertices of degree $d_k = 0$, and three vertices of degree $d_k = 4$, so that $\chi = 1$.

8. Conclusion

In this paper, we recover the conditions for the existence of proper rollings of one surface on another [3–6]—in particular, the condition that the two contact curves, which are generated from the rolling, have identical geodesic curvature. This follows from defining the standard rollings as rigid motions in \mathbb{R}^3 that are conditioned partly via their instantaneous rotation vectors and partly via the obvious condition of contact between the mentioned track curves on the respective surfaces, i.e. a common speed of the contact point along the tracks and common tangent planes at the instantaneous point of contact.

Surfaces are then approximated by a mesh of ribbons. Rolling a surface on a plane and using the Cartan developments of curves allow us to construct developable ribbons that have common tangent planes everywhere along the curve of contact on the surface. In this way, we may approximate the surface not just by one such developable surface but by a full set of ribbons. In short, the surface is ribbonized by flat ribbons which have centre curve contact with the surface. This is a clear difference in comparison with the much used method of triangulations, which typically only give discrete point contact with the surface. In the same way as for triangulations, defining a measure of ‘goodness’ of a Cartan ribbonization is dependent on the actual application. Different methods for designing surfaces by developable patches within a desired global error bound have been developed in [32–35]. For Cartan ribbonizations, this is an interesting problem, which we have addressed by introducing a local measure of goodness for the approximation of the surface along a single ribbon.

Concerning the global structure of the approximations, we present a particularly simple topological inspection of the ribbonized surfaces, which gives the Euler characteristic of the ribbonization—and thence also of the surface, if the ribbonization is fine enough. The ensuing topological formula for the Gauss–Bonnet theorem involves only the vertices of the ribbonization and their degrees. This complements the classical inspections of topology stemming from Morse theory and from the Poincaré–Hopf formula, which also amount to summing over critical point indices. If we organize the ribbonization of a given surface according to level curves of a Morse height function, then we obtain the direct correspondence shown in [table 2](#).

The intriguing relationships between the kinematics of rolling and the geometry of developable surfaces clearly carries many more assets for future work than we cover in the present paper. As indicated above, already the study of ribbonizations could well pave new ways for refined analyses of physical, geometrical and topological properties of surfaces. Not to mention the potentials of their higher dimensional analogues. Possible practical applications are manifold and appear in such diverse fields as robotics, architecture, design, shape analysis and modern engineering; see, for example, the works on rolling spherical robots [36], roof panelling [37], statistical geometric regression analysis [23,24] and the manufacturing of clothes [38].

Data accessibility. The paper has no data or associated material.

Authors' contributions. M.R., J.B. and S.M. planned the research, undertook the research and wrote the manuscript.

Competing interests. We have no competing interests.

Funding. There is no external funding for this paper. All funding comes from the Technical University of Denmark.

Acknowledgements. We thank the referees for their careful reading of the paper and for their helpful comments.

References

- Schumaker LL. 1993 Triangulations in CAGD. *IEEE Comput. Graph. Appl.* **13**, 47–52. (doi:10.1109/38.180117)
- Lawrence S. 2011 Developable surfaces: their history and application. *Nexus Network J.* **13**, 701–714. (doi:10.1007/s00004-011-0087-z)
- Nomizu K. 1978 Kinematics and differential geometry of submanifolds. *Tôhoku Math. J.* **30**, 623–637. (doi:10.2748/tmj/1178229921)
- Kobayashi S, Nomizu K. 1963 *Foundations of differential geometry I*. New York, NY: Interscience Publishers.
- Tunçer Y, Sağel MK, Yayli Y. 2007 Homothetic motion of submanifolds on the plane in \mathbb{E}^3 . *J. Dyn. Syst. Geometr. Theories* **5**, 57–64. (doi:10.1080/1726037X.2007.10698524)
- Cui L, Dai JS. 2010 A Darboux-frame-based formulation of spin-rolling motion of rigid objects with point contact. *IEEE Trans. Robot.* **26**, 383–388. (doi:10.1109/TRO.2010.2040201)
- Molina MG, Grong E. 2014 Geometric conditions for the existence of a rolling without twisting or slipping. *Commun. Pure Appl. Anal.* **13**, 435–452. (doi:10.3934/cpaa.2014.13.435)
- Hananoi S, Izumiya S. 2017 Normal developable surfaces of surfaces along curves. *Proc. R. Soc. Edinb. A* **147**, 177–203. (doi:10.1017/S030821051600007X)
- Izumiya S, Otani S. 2015 Flat approximations of surfaces along curves. *Demons. Math.* **48**, 217–241. (doi:10.1515/dema-2015-0018)
- Raffaelli M, Bohr J, Markvorsen S. 2016 Sculpturing surfaces with Cartan ribbons. In *Bridges 2016: mathematics, music, art, architecture, education, culture* (eds E Torrence, B Torrence, C Séquin, D McKenna, K Fenyves, R Sarhangi), pp. 457–460. Phoenix, AZ: Tessellations Publishing. See <http://archive.bridgesmathart.org/2016/bridges2016-457.pdf>.
- Cui L, Dai JS. 2015 From sliding-rolling loci to instantaneous kinematics: an adjoint approach. *Mech. Mach. Theory* **85**, 161–171. (doi:10.1016/j.mechmachtheory.2014.11.015)
- Chitour Y, Molina MG, Kokkonen P. 2015 Symmetries of the rolling model. *Math. Z.* **281**, 783–805. (doi:10.1007/s00209-015-1508-6)
- Tunçer Y, Ekmekci N. 2010 A study on ruled surface in Euclidean 3-space. *J. Dyn. Syst. Geometr. Theories* **8**, 49–57. (doi:10.1080/1726037X.2010.10698577)
- Chitour Y, Molina MG, Kokkonen P. 2014 The rolling problem: overview and challenges. In *Control theory and sub-Riemannian geometry* (eds G Stefani, JP Gauthier, M Sigalotti, U Boscain, A Sarychev), pp. 103–122. Cham, Switzerland: Springer International Publishing.

15. Krakowski KA, Leite FS. 2016 Geometry of the rolling ellipsoid. *Kybernetika* **52**, 209–223. (doi:10.14736/kyb-2016-2-0209)
16. Sharp J. 2005 D-forms and developable surfaces. In *Renaissance Banff: mathematics, music, art, culture* (eds R Sarhangi, RV Moody), pp. 121–128. Winfield, KS: Bridges Conference. See <http://archive.bridgesmathart.org/2005/bridges2005-121.pdf>.
17. Wills T. 2006 D-forms: 3D forms from two 2D sheets. In *Bridges London: mathematics, music, art, architecture, culture* (eds R Sarhangi, J Sharp), pp. 503–510. London, UK: Tarquin Publications. See <http://archive.bridgesmathart.org/2006/bridges2006-503.html>.
18. Orduño RR, Winard N, Bierwagen S, Shell D, Kalantar N, Borhani A, Akleman EA. 2016 A mathematical approach to obtain isoperimetric shapes for D-form construction. In *Bridges 2016: mathematics, music, art, architecture, education, culture* (eds E Torrence, B Torrence, C Séquin, D McKenna, K Fenyves, R Sarhangi), pp. 277–284. Phoenix, AZ: Tessellations Publishing. See <http://archive.bridgesmathart.org/2016/bridges2016-277.pdf>.
19. Gray A, Abbena E, Salomon S. 2006 *Modern differential geometry of curves and surfaces with Mathematica®*, 3rd edn. Boca Raton, FL: CRC Press.
20. do Carmo MP. 1976 *Differential geometry of curves and surfaces*. Englewood Cliffs, NJ: Prentice Hall.
21. Izumiya S, Saji K, Takeuchi N. 2017 Flat surfaces along cuspidal edges. *J. Singul.* **16**, 73–100. (doi:10.5427/jsing.2017.16c)
22. Singer IM, Thorpe JA. 1967 *Lecture notes on elementary topology and geometry*. New York, NY: Springer.
23. Fletcher PT, Lu CL, Pizer SA, Joshi S. 2004 Principal geodesic analysis for the study of nonlinear statistics of shape. *IEEE Trans. Med. Imaging* **23**, 995–1005. (doi:10.1109/TMI.2004.831793)
24. Hinkle J, Muralidharan P, Fletcher PT, Joshi S. 2012 *Polynomial regression on Riemannian manifolds*. Lecture Notes in Computer Science, vol. 7574, pp. 1–14. Berlin, Germany: Springer.
25. Jupp PE, Kent JT. 1987 Fitting smooth paths to spherical data. *J. R. Stat. Soc. C* **36**, 43–46.
26. Leite FS, Krakowski KA. 2015 Covariant differentiation under rolling maps. Preprint no. 08–22, Universidade de Coimbra, Coimbra, Portugal. (doi:10.1.1.548.718)
27. Sotomayor J, Garcia R. 2008 Lines of curvature on surfaces, historical comments and recent developments. *São Paulo J. Math. Sci.* **2**, 99–143. (doi:10.11606/issn.2316-9028.v2i1p99-143)
28. Ni X, Garland M, Hart JC. 2004 Fair Morse functions for extracting the topological structure of a surface mesh. *ACM Trans. Graph.* **23**, 613–622. (doi:10.1145/1186562.1015769)
29. Milnor JW. 1965 *Topology from the differentiable viewpoint*. Charlottesville, VA: The University Press of Virginia.
30. Milnor JW. 1965 *Morse theory*. Annals of Mathematics Studies 51. Princeton, NJ: Princeton University Press.
31. Barth W, Johannes B, do CMP, Gerd F, Horst K, Jürgen L, Ulrich P, Erhard Q, Helmut R. 1986 *Mathematical models*. Braunschweig, Germany: Friedr. Vieweg & Sohn.
32. Liu Y-J, Lai Y-K, Hu S-M. 2007 Developable strip approximation of parametric surfaces with global error bounds. In *Proc. of Pacific Graphics 2007: 15th Pacific Conf. on Computer Graphics and Applications, Maui, HI, 29 October–2 November 2007*, pp. 441–444. New York, NY: IEEE.
33. Liu Y-J, Lai Y-K, Hu S. 2009 Stripification of free-form surfaces with global error bounds for developable approximation. *IEEE Trans. Autom. Sci. Eng.* **6**, 700–709. (doi:10.1109/TASE.2008.2009926)
34. Tang C, Bo P, Wallner J, Pottmann H. 2016 Interactive design of developable surfaces. *ACM Trans. Graph.* **35**, 1–12. (doi:10.1145/2832906)
35. Rabinovich M, Hoffmann T, Sorkine-Hornung O. 2018 Discrete geodesic nets for modeling developable surfaces. *ACM Trans. Graph.* **37**, 161–1617. (doi:10.1145/3180494)
36. Bai Y, Svinin M, Yamamoto M. 2015 Motion planning for a pendulum-driven rolling robot tracing spherical contact curves. In *Proc. of the IEEE Int. Conf. on Intelligent Robots and Systems, Hamburg, Germany, 28 September–2 October 2015*, pp. 4053–4058. New York, NY: IEEE.
37. Mehrtens P, Schneider M. 2012 Bahn frei für die Architektur—Approximation von Freiform-Flächen durch abwickelbare Streifen. *Stahlbau* **81**, 931–934. Heft 12.
38. Rose K, Sheffer A, Wither J, Cani MP, Thibert B. 2007 Developable surfaces from arbitrary sketched boundaries. In *Proc. of the Eurographics Symp. on Geometry Processing (2007), Barcelona, Spain, 4–6 July 2007* (eds AG Belyaev, M Garland), pp. 163–172. Aire-la-Ville, Switzerland: The Eurographics Association.